

# Modeling Recent Climate Variability in the Arctic Ocean

W. Maslowski<sup>1</sup>, B. Newton<sup>2,3</sup>, P. Schlosser<sup>2,3</sup>, A. Semtner<sup>1</sup>, D. Martinson<sup>2</sup>

**Abstract.** Dramatic changes in the circulation of sea ice and the upper layers of the Arctic Ocean have been reported during the last decade. Similar variability is modeled using a regional, coupled ice-ocean model. Realistic atmospheric forcing fields for 1979-93 are the only interannual signal prescribed in the model. Our results show large-scale changes in sea ice and oceanic conditions when comparing results for the late 1970s / early 1980s and the 1990s. We hypothesize that these changes are in response to even larger scale atmospheric variability in the Northern Hemisphere that can be defined as either the Arctic Oscillation or the North Atlantic Oscillation. Agreement between the direction and scale of change in the model and observations, in the absence of interannual forcing from the global ocean thermohaline circulation, suggests that the atmospheric variability by itself is sufficient to produce basin-scale changes in the Arctic Ocean and sea ice system.

## 1. Introduction

In recent years, several authors have identified a dramatic shift in hydrographic fronts within the Central and Eastern Arctic Ocean [Carmack *et al.*, 1995; McLaughlin *et al.*, 1996; Morison *et al.*, 1998; Steele and Boyd, 1998; Ekwurzel *et al.*, 2000]. A boundary between halocline waters with and without Pacific influence has shifted from approximately along the Lomonosov Ridge to the Mendeleev and Alpha ridges. Simultaneously, Atlantic-derived water has significantly increased its presence in the eastern Arctic. This oceanic shift has been associated with a reorganization of the large-scale sea ice drift, including a shrinkage of the Beaufort Gyre and the eastward deflection of the Transpolar Drift [Kwok, 2000]. Such changes may have significant effect on heat, sea ice and fresh water budgets of the Arctic Ocean. In our numerical experiment, we apply daily-averaged atmospheric forcing derived from the European Centre for Medium-range Weather Forecasts (ECMWF) reanalyzed fields for 1979-93 to a high resolution, coupled ice-ocean model to determine the role of Pan-Arctic atmospheric circulation and its variability in driving changes in the Arctic Ocean.

## 2. Model Description

We use a limited-domain coupled Arctic Ocean and sea ice general circulation model. The ocean model is based

<sup>1</sup>Department of Oceanography, Naval Postgraduate School, Monterey, CA.

<sup>2</sup>Lamont-Doherty Earth Observatory, Columbia University, Palisades, NY.

<sup>3</sup>Also at Department of Earth and Environmental Sciences, Columbia University, Palisades, NY.

Copyright 2000 by the American Geophysical Union.

Paper number 1999GL011227.  
0094-8276/00/1999GL011227\$05.00

on the GFDL formulation adapted for parallel computers [Smith *et al.*, 1992]. The rotated numerical grid covers the Arctic Ocean, the sub-polar seas and the North Atlantic to approximately 50° N (Plate 1). The Bering Strait is closed. No mass flux is allowed through the closed lateral boundaries. The grid is relatively fine (~18 km and 30 levels) but it is not eddy resolving in the Arctic Ocean, where the Rossby radius is 5-10 km. Such a resolution, combined with a free-surface approach allows retention of unsmoothed bathymetry and realistic coastlines. Many mesoscale bathymetric features, important to large-scale ocean and sea-ice circulation, water mass formation, shelf-basin and inter-basin communication, are included in the model. The non-linear Navier-Stokes equations are solved in spherical form. Hydrostatic balance is assumed. Laplacian diffusivity and viscosity in the vertical direction and biharmonic in the horizontal are used. More details about the ocean model can be found in Smith *et al.*, [1992].

The ice model is a version of the Hibler [1979] viscous-plastic, dynamic-thermodynamic ice model, adapted for parallel computers. A linear vertical profile of temperature within the ice [Semtner, 1976] and the freezing point at the ocean-ice interface are assumed. At the ice surface, heat flux is calculated according to the energy budget, as in Parkinson and Washington [1979]. The surface energy budget is calculated using the ECMWF data, including the shortwave radiation, cloud cover and 2-m air temperature and dew-point. Downward longwave radiation was calculated from 2-m air temperature and cloud cover. Horizontal stress at the surface was calculated from the ECMWF 10-m wind fields. Using this forcing, the model has been shown to give realistic distributions of sea ice properties [Zhang *et al.*, 1999].

## 3. The Experiment

The atmospheric forcing is applied to the sea ice, which transfers momentum, heat and buoyancy fluxes to the ocean. Where ice thickness is zero, the surface momentum and thermodynamic fluxes are applied directly to the ocean. Surface temperature and salinity are restored toward the Levitus monthly climatology, with a time scale of 1 year and 4 months, respectively.

The model includes freshwater inflows from the major Arctic rivers (Mackenzie, Dvina, Pechora, Ob, Yenisey, Kotuy, Lena, Indigirka and Kolyma) and the Bering Strait. No mass is exchanged there, but daily averages of the river runoff and Bering Strait inflow are used to recalculate the salinity and temperature in their source regions, and act as a freshwater source to the model domain. In addition to their contribution to the density calculation, the freshwater inflows are also tracked as separate “dye” tracers. Similarly, any water moving northward across the Greenland-Iceland-Scotland Ridge is marked with an “Atlantic” dye. The fresh-

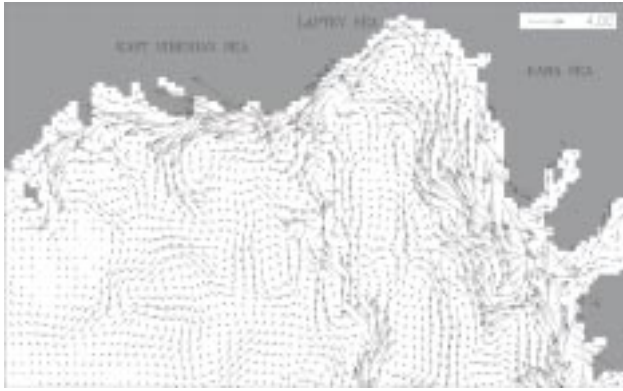


**Figure 1.** Velocity difference (cm/s) averaged over depth of 180–560 m between the 3-year mean of 1991–93 and the mean of last 3 years of the 20-year spinup using 1979 forcing. Every 2nd vector in each direction is shown.

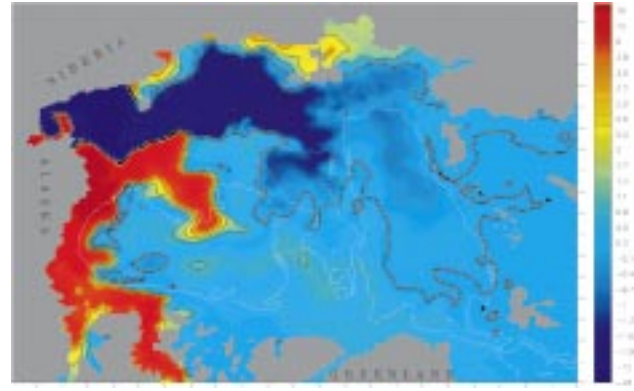


**Plate 2.** Difference in concentration (%) of the Bering Strait Inflow tracer at 0–20 m between the end of 1993 and 1979 after 20-year spinup. Negative values track retreat of Pacific Water.

water and Atlantic dye tracers are not restored at the surface. Together, these tracers allow us to track the main sources of distinct water types in the Arctic: Atlantic and Pacific inflows and waters formed over the Arctic shelves.

We report here on the current experiment as it clearly demonstrates the significance of regional atmospheric forcing over the northern high latitudes in driving large-scale, decadal changes in the sea ice–ocean system. In addition, absence of the interannual thermohaline communication with the global ocean allows us to separate the wind- versus thermohaline-driven effects in the Arctic Ocean response to climate change. The experiment begins with a 20-year spinup of the model, forced by the repeated 1979 ECMWF annual cycle and climatological freshwater data. It was initialized from our earlier 200-year integration using 1990–94 ECMWF forcing. After the spinup, the model evolves under the 1979–93 atmospheric data. The tracers are integrated, starting from zero, throughout the 35-year experiment. The large-scale circulation patterns in the upper ocean do not change significantly during the second decade of the 20-year spinup nor during an additional 15-year run with 1979 forcing as a reference.

## 4. Results

During the 20-year spinup, the core of Atlantic inflow roughly follows the pathways documented by *Schauer et al.*, [1997]. Atlantic Water dye enters the Barents shelf mainly via the Bear Island Trough and also via the Norwegian Coastal Current. It exits along the eastern flank of the St. Anna Trough and a few smaller troughs (Voronin to the east and Franz-Victoria to the west). At the shelf-break it merges with a branch of dye that has propagated northward through Fram Strait and then eastward along the northern shelf-break of the Barents Sea. The combined signal propagates as a narrow boundary current along the continental slope with the shallow water to the right. During the second decade of the 20-year spinup (and the additional 15-year run with 1979 forcing) the circulation patterns of the Atlantic dye do not change significantly, although concentrations continue to rise throughout the Eurasian Basin.

After 20 years of repeated 1979 forcing, the tracer flows east along the slope towards the Lomonosov Ridge, and then northward along the Eurasian flank of the ridge to exit via Fram Strait into the Greenland Sea (Plate 1a). Over the

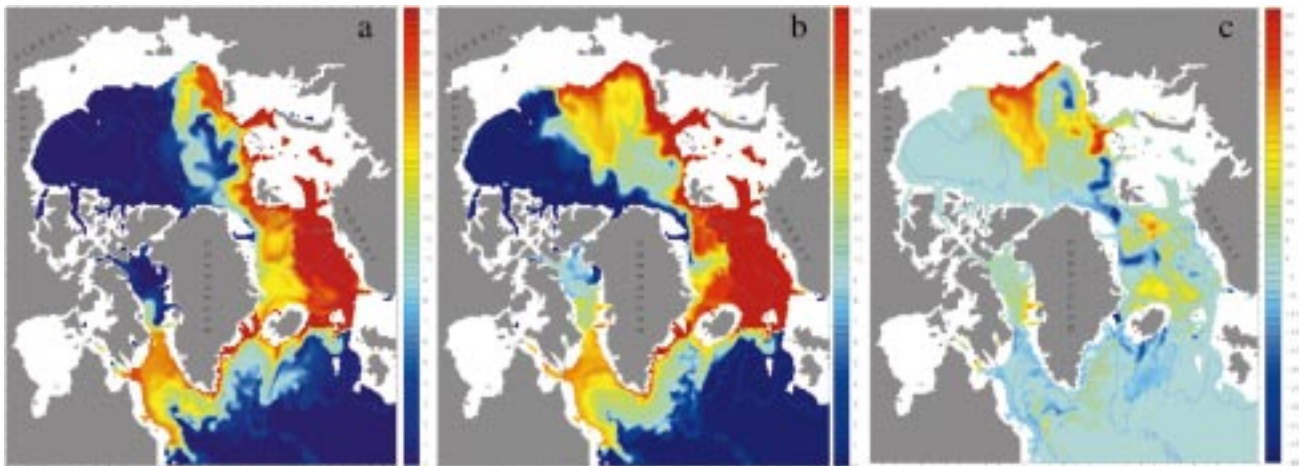


**Plate 1.** Concentration of Atlantic Water tracer (%) averaged over depth of 180–560 m (a) after repeating the 1979 cycle for 20 years, (b) in December 1993 (15 years later) and (c) difference between the 1993 and 1979 concentrations. Contour line represents the 2500-m isobath.

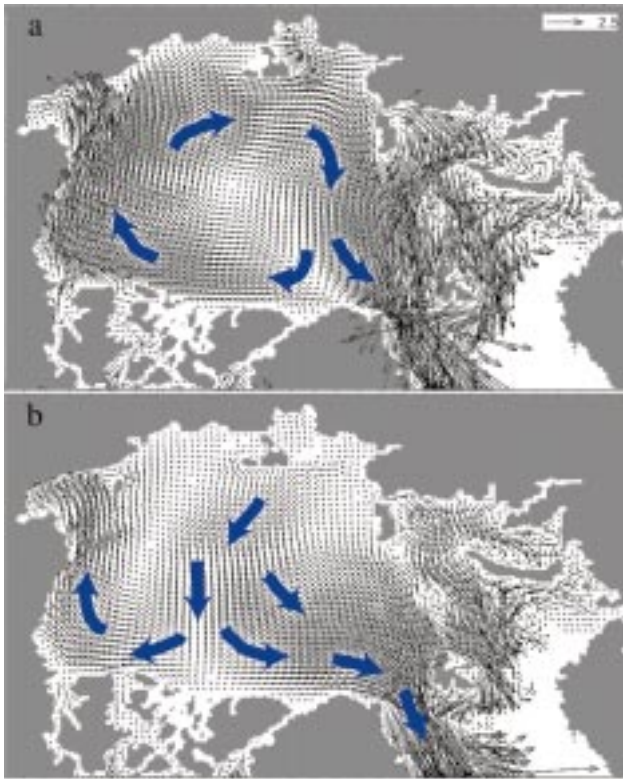


**Plate 3.** Mean sea ice drift (cm/s) in (a) 1979 at the end of spinup and in (b) 1990-93. Every  $3^\circ d$  vector in each direction is shown.

open ocean, away from the boundary current, the Atlantic dye bifurcates in the vertical direction. A thin layer of high dye concentration (20-60%) is present in the surface waters. This marks inflowing Atlantic water, which has been freshened by the relaxation to possibly resemble Nansen Basin surface water, and which has joined the Arctic surface circulation. There is very little Atlantic dye in the halocline, and the dye concentration is high (20-40%) in the model's Atlantic Layer ( $\sim 300$ -1000 meters). Within this layer, the dye penetrates most efficiently down to  $\sim 800$  m. By the end of the spinup, the subsurface (below 100 m) dye is nearly contained in the Eurasian Basin. There is a minor leakage into the Canadian Basin, where the Lomonosov Ridge joins the Siberian shelf, and further north, near the Pole. At all depths, the Atlantic dye distribution indicates a cyclonic circulation in the Eurasian basin, with a dye concentration maximum marking a slow northward jet along the Eurasian flank of the Lomonosov Ridge.

Following the use of 1979-93 forcing, the Atlantic tracer has crossed the Lomonosov Ridge, and flows primarily along the Siberian shelf-break in the Makarov Basin, as far east as the Arlis Plateau (Plate 1b). The tracer propagates northward in two plumes, one along the Mendeleev Ridge and the other along the Canadian flank of the Lomonosov Ridge. In the northern end of the Makarov Basin, these plumes diffuse, and the signal spreads throughout the Makarov Basin. Meanwhile, the Atlantic dye concentration on the Eurasian flank of the Lomonosov Ridge continues to grow, but significantly slower. The difference in distribution of the Atlantic dye between 1993 and 1979 shown in Plate 1c indicates where accumulation of Atlantic Water has occurred. The

concentrations along the Eurasian flank have largely stabilized, and are well below the concentrations on the Canadian side. Thus, the area of maximum concentration, away from the shelf and slope regions, has shifted from the Amundsen to the Makarov Basin. This redistribution of tracer is qualitatively in agreement with observations of Atlantic Water from the SCICEX submarine cruises, as cited above. It also agrees with warm water trends derived from the Arctic'91 and AOS'94 cruise data over the Lomonosov Ridge. Finally, it agrees with the direction and scale of the shift observed in the Larsen-93 data, except that *McLaughlin et al.*, [1996] document the Atlantic Layer waters leading the surface in trending eastward across the Makarov Basin. In our model, the shift is fairly uniform in the vertical, with the surface waters leading somewhat.

Analysis of the velocity fields at Atlantic Layer depth reveals that the northward jets along the Lomonosov and Mendeleev ridges are present both during the spinup and toward the end of experiment. The change in distribution of the Atlantic tracer can be explained by the depth-averaged (180-560m) velocity difference between the mean circulation of the 1990s and 1979 (Figure 1). It appears that under the influence of the interannual forcing, a much stronger along-slope current develops at the northern edge of the Kara, Laptev and East Siberian seas, advecting the Atlantic tracer past the Lomonosov Ridge and into the Makarov Basin.

A similar change is evident from the Bering Strait inflow (BSI) tracer distribution. This is in particular relevant to the Atlantic-Pacific front shift in the halocline. By the end of spinup, the BSI dye has flooded the Russian shelves as far as the Laptev Sea. There it turns northward with the Transpolar Drift flowing towards Fram Strait. By the end of 1993, it leaves the Chukchi shelf via two pathways: one along the Alaskan North Slope entering the Canadian Archipelago and the other along the Chukchi Plateau meandering across the Beaufort Sea toward Fram Strait. The change between 1993 and 1979 (Plate 2) is consistent with the observed retreat of Pacific Water from the Makarov Basin.

## 5. Discussion

In the model, the only interannual forcing is prescribed with the atmospheric fields. To compare atmospheric regimes from ECMWF data we have calculated the difference between the cold-month (DJFM) sea level pressure fields for 1991-93 and 1979-81 (not shown). The resulting pattern corresponds to the Northern Hemisphere oscillation identified in various data sets by many authors [e.g. *Hurrell*, 1996; *Thompson and Wallace*, 1998; *Walsh et al.*, 1996]. Temperature and salinity fields at the surface, along the lateral boundaries, and in the river inflows are from climatologies. In addition, interannual changes in the thermodynamic forcing from the atmosphere are damped by the surface ocean relaxation to climatology. Therefore, we interpret our results mainly as a response to changes in the surface wind stress.

The effect of a cyclonic shift in the surface winds is clearly visible in the sea ice drift. Plate 3 shows the mean sea-ice pattern from the year 20 of model spinup and from the last 4 years of the experiment. In 1979 (Plate 3a), the Beaufort Gyre extends over the entire Canadian Basin and the Transpolar Drift is positioned along the Laptev Sea - Fram Strait axis. In the 1990s (Plate 3b) the Beaufort Gyre becomes

much smaller and it is confined mostly within the Beaufort Sea. This change is associated with an eastward deflection of the Transpolar Drift, to the northern boundary of the Beaufort Sea.

We suggest the following chain of events to explain the large-scale changes in sea ice and upper ocean circulation. Variability in the Northern Hemisphere weather patterns has resulted in a lower time-mean sea-level pressure and an increased storminess activity over the Arctic Ocean in the late 1980s and 1990s. This has established a more divergent, cyclonic circulation of sea ice, most noticeable in the Makarov Basin. Through Ekman pumping, the ice-ocean stress will cause a negative sea surface height anomaly in the central Arctic and positive anomaly outside this region. The resulting geostrophic flow is cyclonic and barotropic accelerating the shelf and slope currents to the east, especially in the Russian sector of the Arctic Ocean. Atlantic and freshwater dyes which, in the spinup, would exit the shelf and slope regions on the Eurasian side of the Lomonosov Ridge are advected over the ridge and spread northward mainly in the Makarov Basin.

Our basic agreement with findings by *Proshutinsky and Johnson* [1997] about the importance of wind forcing on the surface Arctic Ocean circulation suggests that the mechanism may be robust, and merits further investigation.

**Acknowledgments.** Maslowski and Semtner are supported by grants from NSF Arctic System Science, the DOE Climate Change Prediction Program, and Cray Research Inc. via the Univ. of Alaska. Schlosser and Newton have been supported by grants: ONR/AASERT N00014-96-1-0612 and NSF/OPP 97-08924. LDEO contribution 6085. Computer resources have been provided by the Arctic Region Supercomputing Center through the DOD High Performance Computer Modernization Program. We also thank the reviewers of this manuscript for helpful suggestions.

## References

- Carmack, E.C., R.W. Macdonald, R.G. Perkin, F.A. McLaughlin and R.J. Pearson, Evidence for warming of Atlantic Water in the Southern Canadian Basin of the Arctic Ocean: Results from the Larsen-93 Expeditions, *Geophys. Res. Lett.*, *22*(9), 1061-1064, 1995.
- Ekwurzel, B., P. Schlosser, J. Swift, R. Mortlock and R. Fairbanks, River runoff, sea ice meltwater, and Pacific water dis-

- tribution and mean residence times in the Arctic Ocean, *J. Geophys. Res.*, *submitted*, 2000.
- Hibler, W.D. III, A dynamic thermodynamic sea ice model, *J. Phys. Oceanogr.*, *9*, 815-846, 1979.
- Hurrell, J., Influence of variations in extratropical wintertime teleconnections on Northern Hemisphere temperature, *Geophys. Res. Lett.*, *23*(6), 665-668, 1996.
- Kwok, R., Recent changes in the Arctic Ocean sea ice motion associated with the North Atlantic oscillation, *Geophys. Res. Lett.*, *27*(6), 775-778, 2000.
- McLaughlin, F.A., E.C. Carmack, R.W. Macdonald, and J.K.B. Bishop, Physical and geochemical properties across the Atlantic/Pacific water mass front in the southern Canadian Basin, *J. Geophys. Res.*, *101*(C1), 1183-1197, 1996.
- Morison, J., M. Steele, and R. Andersen, Hydrography of the upper Arctic Ocean measured from the nuclear submarine U.S.S. Pargo, *Deep Sea Res.*, *45*(1), 15-38, 1998.
- Parkinson, C.L., and W.M. Washington, A large-scale numerical model of sea ice, *J. Geophys. Res.*, *84*, 311-337, 1979.
- Proshutinsky, A.Y., and M.A. Johnson, Two circulation regimes of the wind-driven Arctic Ocean, *J. Geophys. Res.*, *102*, 12,493-12,514, 1997.
- Schauer, U., R.D. Muench, B. Rudels, and L. Timokhov, Impact of eastern Arctic shelf waters on the Nansen Basin intermediate layers, *J. Geophys. Res.*, *102*, 3371-3382, 1997.
- Semtner, A.J. Jr., A model for the thermodynamic growth of sea ice in numerical investigations of climate, *J. Phys. Oceanogr.*, *6*, 379-389, 1976.
- Steele, M. and T. Boyd, Retreat of the cold halocline layer in the Arctic Ocean, *J. Geophys. Res.*, *103*(C5), 10,419-10,435, 1998.
- Smith, R.D., J.K. Dukowicz, and R.C. Malone, Parallel ocean general circulation modeling, *60*, 38-61, 1992.
- Thompson, D.W.J. and J.M. Wallace, Arctic Oscillation signature in the wintertime geopotential height and temperature fields, *Geophys. Res. Lett.*, *25*(9), 1297-1300, 1998.
- Walsh, J.E., W.L. Chapman and T.L. Shy, Recent decrease of sea level pressure in the Central Arctic, *9*, 480-486, 1996.
- Zhang, Y., W. Maslowski, and A.J. Semtner, Impact of mesoscale ocean currents on sea ice in high resolution Arctic ice and ocean simulations, *J. Geophys. Res.*, *104*(C8), 18,409-18,430, 1999.

---

W. Maslowski and A. Semtner, Department of Oceanography, Naval Postgraduate School, 833 Dyer Road, Monterey, CA 93943, USA. (e-mail: maslowsk@ucar.edu; sbert@ucar.edu)

D. Martinson, B. Newton, and P. Schlosser, Lamont-Doherty Earth Observatory, Columbia University, Palisades, NY 10964, USA. (e-mail: dgm@ldeo.columbia.edu; bnewton@ldeo.columbia.edu; peters@ldeo.columbia.edu)

(Received November 14, 1999; accepted June 5, 2000)